

# Calculation and experimental validation of spectral properties of microsize grains surrounded by nanoparticles

Haitong Yu,<sup>1</sup> Dong Liu,<sup>1</sup> Yuanyuan Duan,<sup>1,\*</sup> and Xiaodong Wang<sup>2,3</sup>

<sup>1</sup> Key Laboratory for Thermal Science and Power Engineering of MOE, Beijing Key Laboratory for CO<sub>2</sub> Utilization and Reduction Technology, Tsinghua University, Beijing 100084, China

<sup>2</sup> State Key Laboratory of Alternate Electrical Power System with Renewable Energy Sources, North China Electric Power University, Beijing 102206, China

<sup>3</sup> Beijing Key Laboratory of Multiphase Flow and Heat Transfer for Low Grade Energy, North China Electric Power University, Beijing 102206, China

\*yyduan@mail.tsinghua.edu.cn

**Abstract:** Opacified aerogels are particulate thermal insulating materials in which micrometric opacifier mineral grains are surrounded by silica aerogel nanoparticles. A geometric model was developed to characterize the spectral properties of such microsize grains surrounded by much smaller particles. The model represents the material's microstructure with the spherical opacifier's spectral properties calculated using the multi-sphere T-matrix (MSTM) algorithm. The results are validated by comparing the measured reflectance of an opacified aerogel slab against the value predicted using the discrete ordinate method (DOM) based on calculated optical properties. The results suggest that the large particles embedded in the nanoparticle matrices show different scattering and absorption properties from the single scattering condition and that the MSTM and DOM algorithms are both useful for calculating the spectral and radiative properties of this particulate system.

© 2014 Optical Society of America

**OCIS codes:** (030.5620) Radiative transfer; (160.6060) Solgel; (290.4210) Multiple scattering.

---

## References and links

1. J. Kuhn, T. Gleissner, M. C. Arduinischester, S. Korder, and J. Fricke, "Integration of mineral powders into SiO<sub>2</sub> aerogels," *J. Non-Cryst. Solids* **186**, 291–295 (1995).
2. J. Zhao, Y. Duan, X. Wang, and B. Wang, "Effects of solid-gas coupling and pore and particle microstructures on the effective gaseous thermal conductivity in aerogels," *J. Nanopart. Res.* **14**(8), 1–15 (2012).
3. J. Fricke and T. Tillotson, "Aerogels: production, characterization, and applications," *Thin Solid Films* **297**(1-2), 212–223 (1997).
4. J. Zhao, Y. Duan, X. Wang, X. Zhang, Y. Han, Y. Gao, Z. Lv, H. Yu, and B. Wang, "Optical and radiative properties of infrared opacifier particles loaded in silica aerogels for high temperature thermal insulation," *Int. J. Therm. Sci.* **70**, 54–64 (2013).
5. X. Wang, D. Sun, Y. Duan, and Z. Hu, "Radiative characteristics of opacifier-loaded silica aerogel composites," *J. Non-Cryst. Solids* **375**, 31–39 (2013).
6. V. Napp, R. Caps, H. P. Ebert, and J. Fricke, "Optimization of the thermal radiation extinction of silicon carbide in a silica powder matrix," *J. Therm. Anal. Calorim.* **56**(1), 77–85 (1999).
7. J. M. Dlugach, M. I. Mishchenko, and D. W. Mackowski, "Scattering and absorption properties of polydisperse wavelength-sized particles covered with much smaller grains," *J. Quant. Spectrosc. Radiat. Transf.* **113**(18), 2351–2355 (2012).
8. C. Tien and B. L. Drolen, "Thermal Radiation in Particulate Media with Dependent and Independent Scattering," in *Annual Review of Numerical Fluid Mechanics and Heat Transfer*, T. C. Chawla, ed. (Hemisphere, 1987).
9. M. I. Mishchenko, "Electromagnetic scattering by a fixed finite object embedded in an absorbing medium," *Opt. Express* **15**(20), 13188–13202 (2007).
10. M. I. Mishchenko, "Multiple scattering by particles embedded in an absorbing medium. I. Foldy-Lax equations, order-of-scattering expansion, and coherent field," *Opt. Express* **16**(3), 2288–2301 (2008).
11. H. Yu, D. Liu, Y. Duan, and X. Wang, "Theoretical model of radiative transfer in opacified aerogel based on realistic microstructures," *Int. J. Heat Mass Tran.* **70**, 478–485 (2014).

12. D. W. Mackowski and M. I. Mishchenko, "A multiple sphere T-matrix Fortran code for use on parallel computer clusters," *J. Quant. Spectrosc. Radiat. Transf.* **112**(13), 2182–2192 (2011).
13. W. A. Fiveland, "Discrete ordinate methods for radiative heat transfer in isotropically and anisotropically scattering media," *J. Heat Transfer-Trans. ASME* **109**(3), 809–812 (1987).
14. T. A. Witten, Jr. and L. M. Sander, "Diffusion-limited aggregation, a kinetic critical phenomenon," *Phys. Rev. Lett.* **47**(19), 1400–1403 (1981).
15. A. Emmerling and J. Fricke, "Scaling properties and structure of aerogels," *J. Sol-Gel Sci. Techn.* **8**, 781–788 (1997).
16. M. I. Mishchenko, L. Liu, and G. Videen, "Conditions of applicability of the single-scattering approximation," *Opt. Express* **15**(12), 7522–7527 (2007).
17. C. F. Bohren and D. R. Huffman, *Absorption and Scattering of Light by Small Particles* (Wiley, 1983).
18. E. D. Palik, ed., *Handbook of Optical Constants of Solids* (Academic, 1985).
19. S. Lallich, F. Enguehard, and D. Baillis, "Experimental determination and modeling of the radiative properties of silica nanoporous matrices," *J. Heat Transfer-Trans. ASME* **131**(8), 082701 (2009).
20. A. Tamanai, H. Mutschke, J. Blum, and R. Neuhäuser, "Experimental infrared spectroscopic measurement of light extinction for agglomerate dust grains," *J. Quant. Spectrosc. Radiat. Transf.* **100**(1-3), 373–381 (2006).

## 1. Introduction

Opacified aerogels (Fig. 1(a)) are porous materials with ultra-low thermal conductivities which are composed by the silica aerogel (porosity  $\geq 90\%$ ) and opacifier grains [1]. The aerogel consists of packed silica nanoparticles (diameters  $d = 5\text{-}50\text{ nm}$ ) [2,3]. The opacifiers are mineral grains with large scattering and/or absorption efficiencies in the near-infrared to enhance the aerogel's extinction coefficients for thermal radiation to achieve low thermal conductivities at high temperatures [1]. Opacifier grains usually have diameters of  $1\text{-}5\text{ }\mu\text{m}$  and occupy only a small volume fraction ( $\approx 1.5\%$ ) in the material to maintain the material's high porosity (Fig. 1(b)).

Accurate calculations of the opacifier's optical properties are important for predicting and optimizing the material's insulation ability. Materials with large spectral extinction coefficients tend to have low radiative flux intensities, while materials with large albedo and strong backward scattering tend to absorb less energy and are resistant to overheating caused by thermal impact. In opacified aerogels, the optical properties of the micrometer-sized opacifier particles are influenced by the surrounding nanoparticles. Scattering interactions exist between the opacifier and the aerogel, but the refraction and scattering of silica is so weak in the near infrared that the aerogel's influence on the opacifier's radiative properties have been neglected by most studies [4–6] which have mainly characterized the opacified aerogels' extinction coefficient with the single scattering model. Neither have been other optical properties such as the spectral albedo and the phase functions studied in detail in these studies. Dlugach et al. [7] calculated the small particles influence on the optical properties of a larger particle, but the sizes, geometries and optical constants were very different from the case of opacified aerogels.

The significant difference in sizes and spatial distributions of aerogel and opacifier particles prohibits characterization by simple dependent scattering models [8]. Approximating this problem as particle scattering in an effective absorbing media [9,10] is also not rigorous because it neglects the scattering by aerogel particles. A recent work by Yu et al. [11] generated a geometric model to represent the material microstructure and used the multiple-sphere T-matrix (MSTM) algorithm [12] to characterize the extinction coefficient and the radiative conductivity. The present work analyzes the surrounding nanoparticles' influence on the spectral properties of a large particle in more detail by characterizing the spectral properties including the extinction coefficient, albedo and phase function. The results of this theoretical model are validated by comparing the experimental measured reflectance with the solution for radiative transfer equation (RTE) in an opacified aerogel slab with the 1-D discrete ordinate method (DOM) [13] using optical properties calculated by MSTM algorithm.

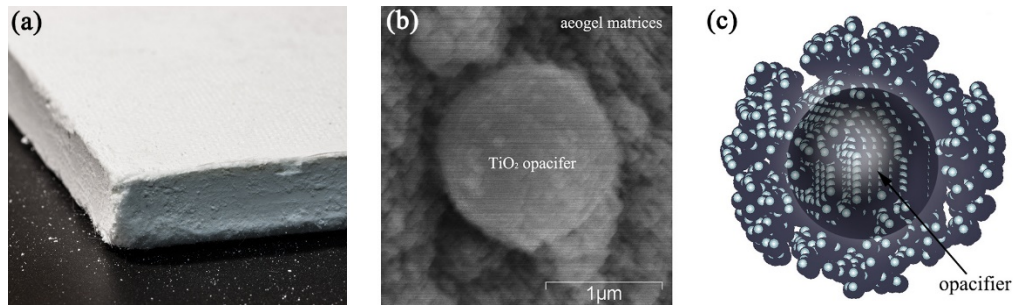


Fig. 1. TiO<sub>2</sub> opacified aerogels: (a) monolithic slab sample; (b) SEM picture of an opacifier grain surrounded by the aerogel; (c) geometric model used in the MSTM calculations.

## 2. Theoretical model

This work used TiO<sub>2</sub> opacified aerogel samples with apparent densities of 300-350 kg·m<sup>-3</sup>. The TiO<sub>2</sub> opacifier (rutile type) with diameters of 1-3 μm had a 20% weight fraction in the material. SEM pictures (Fig. 1(b)) show that the opacifier particles are approximately spherical and are surrounded by aerogel nanoparticles. The opacifier surface is partly exposed in the image because of damage caused by the SEM sample preparation.

The opacified aerogel's microstructure can be described by diffusion-limited aggregation (DLA) [14] which simulate the sol-gel process of aerogel preparation and generate aggregates with similar fractal dimensions as the aerogel [15]. In this work, a spherical TiO<sub>2</sub> particle was used as the original seed particle and then, according to the DLA algorithm, silica nanoparticles were cast into the volume region and attached to the previous particle surfaces [11]. The volume for the aerogel aggregate generation was determined from the average space of one opacifier grain in the actual material. The number of particles was increased until casting more aerogel particles onto the structure will not further influence optical properties of the opacifier. The resulting structure (Fig. 1(c)) contained more than 3000 aerogel nanoparticles with only a single opacifier grain because the opacifier volume fraction is so small that scattering of multiple opacifier grains can be modeled by the single scattering approximation [16].

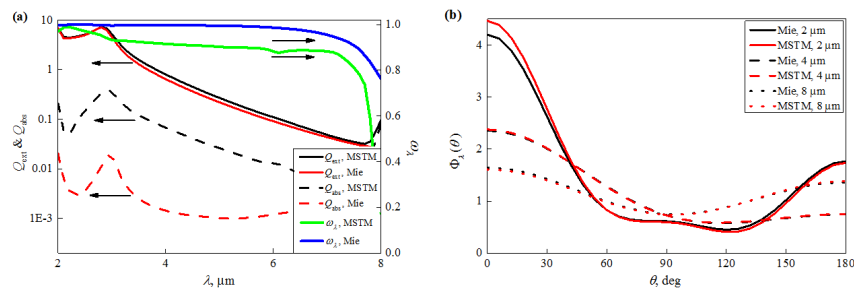


Fig. 2. Calculated TiO<sub>2</sub> opacifiers optical properties: (a) extinction efficiency,  $Q_{\text{ext}}$ , absorption efficiency,  $Q_{\text{abs}}$ , and scattering albedo,  $\omega_s$ , and (b) phase functions,  $\Phi_1$ , at 2 μm, 4 μm and 8 μm.

After the geometry was generated, the spectral properties of a TiO<sub>2</sub> sphere ( $d = 1 \mu\text{m}$ ) surrounded by silica nanoparticles were calculated using the multi-sphere T-matrix (MSTM) code [12], a numerically accurate method capable of parallel computations for large numbers of spheres with extreme size difference. The MSTM results were compared with the single scattering solutions (Mie theory) [17]. The optical constants of rutile and silica are from the HOC by Palik [18]. Figure 2(a) shows that in the 2-8 μm range, the aerogel particles only weakly influence the opacifier's extinction efficiency but increase its absorption efficiency by an order of magnitude and decrease its albedo. Thus the aerogel nanoparticles boost the absorption of the opacifier grains which results in stronger total absorption and weaker

scattering of thermal radiation. The phase functions  $\Phi_\lambda$  given by the MSTM code and by Mie theory for several wavelengths are almost identical (Fig. 2(b)), possibly because the aerogel particles are nearly isotropically distributed and do not alter the opacifier's scattered energy distribution.

### 3. Reflectance prediction and experimental validation

The computed optical properties in Fig. 2 can be validated by reflectance and/or transmittance measurement of slab samples. Previous studies [1,19] simultaneously measured the aerogel's spectral reflectance and transmittance to determine the extinction coefficient and the albedo through an inverse solution of the RTE. The difficulty of this method lies in the transmittance measurement, as opacified aerogels are designed to have very high near infrared extinction. Very thin aerogel films with observable transmittance are difficult to create due to the material's lack of mechanical strength. Even with thin films obtained, the uncertainty and inconsistency of their thickness compromises the measurement accuracy. One possible solution is to grind monolithic samples into grains and tableting them with large amounts of transparent KBr powder to increase the transmittance. However, the grinding and tableting damage its microstructure and therefore change the actual spectral properties of the opacified aerogel. Tamanai et al. [20] also pointed out that the measured optical properties of a dispersed sample were influenced by the KBr medium. Moreover, this method requires an inverse solution of the RTE by approximation methods (such as the diffusion approximation or the transport approximation) [19] which further affects the results' accuracy.

The reflectance of opacified aerogels is more observable than the transmittance and is insensitive to the sample thickness for an optically thick slab. However, various optical properties such as the extinction, albedo and phase functions cannot be determined from only the measured reflectance. Therefore, instead of deriving the spectral properties from measurements, the calculated spectral parameters were used here in the RTE to predict the sample reflectance for comparison with measurements. The discrete ordinate method (DOM) [13] was used to solve the RTE. Compared to approximations used, the DOM characterizes the scattering phase function's influence in finer detail.

The RTE for a one dimensional participating media without thermal emission is written as:

$$\mu \frac{dI_\lambda(z, \mu)}{\beta_\lambda dz} = -I_\lambda(z, \mu) + \frac{\omega_\lambda}{2} \int_{-1}^1 \Phi_\lambda(\mu, \mu') I(z, \mu') d\mu' \quad (1)$$

where  $z$  is the coordinate along the sample thickness and  $\mu = \cos\theta$  indicates the scattering direction. The input spectral parameters are the extinction coefficient,  $\beta_\lambda$ , the scattering albedo,  $\omega_\lambda$ , and the phase function,  $\Phi_\lambda$ . The directional, spectral radiative intensity along  $z$ -axis,  $I_\lambda$ , is determined from the RTE and the boundary conditions at the sample surfaces:

$$I_\lambda(z=0, \mu) = \begin{cases} I_0 & (|\mu - \mu_0| < \varepsilon) \\ 0 & (\mu > 0, \mu \neq \mu_0) \end{cases}, I_\lambda(z=h, \mu) = 0 \text{ for } \mu \leq 0 \quad (2)$$

where  $\mu_0 > 0$  is determined by the incidence direction in the experiment,  $\varepsilon$  denotes the small angle region where the incidence intensity  $I_0$  exists and  $h$  is the sample thickness. The hemispherical reflectance,  $R_\lambda$ , is defined as the ratio of the total reflected energy to the incident energy at  $z = 0$ :

$$R_\lambda = -\int_{-1}^0 I_\lambda(z=0, \mu) \mu d\mu / \int_0^1 I_\lambda(z=0, \mu) \mu d\mu \quad (3)$$

To solve the RTE, the DOM replaces the angular integral term in Eq. (1) by quadrature [13]:

$$\int_{-1}^1 \mu \Phi(\mu) d\mu \approx \sum_{k=1}^N w_k \mu_k \Phi(\mu_k) \quad (4)$$

where  $N$  is the number of quadrature points in  $\mu \in [-1, 1]$  and the discrete angular ordinates,  $\mu_k$ , and their weights,  $w_k$ , are determined by Fiveland ( $S_N$  approximation) [13] as

$$\begin{cases} w_k = 2/N & (k = 1, 2, \dots, N) \\ \int_0^1 \mu^i d\mu = \sum_{k=1}^{N/2} w_k \mu_k^i & (i = 0, 1, \dots, N/2) \end{cases} \quad (5)$$

The discrete ordinates and the weights are used to write the RTE in Eq. (1) into a group of  $N$  equations. The equation for the  $k$ th direction

$$\mu \frac{dI_\lambda(z, \mu_k)}{\beta_\lambda dz} = -I_\lambda(z, \mu_k) + \frac{\omega_\lambda}{2} \sum_{k'=1}^N \Phi_\lambda(\mu_k, \mu_{k'}) I_\lambda(z, \mu_{k'}) w_{k'} \quad (6)$$

describes the radiative intensity in direction  $\mu_k$ . The complete RTE can then be solved numerically by replacing the spatial differential  $dI_\lambda/dz$  with a finite difference. This reflectance prediction procedure is independent of any previous optical measurements with only optical constants from the literature and sample gradients parameters needed.

The spectral hemispherical reflectance of the opacified aerogel was measured with a Bruker FTIR spectrometer and a gold integration sphere with near normal incident light. Measured wavelength region was 2.0 to 16.7  $\mu\text{m}$  with the short wavelength results (2-8  $\mu\text{m}$ ) as the main concern to be compared with the DOM results. The actual opacifiers were not monodisperse particles with the diameters of the  $\text{TiO}_2$  opacifier in the sample being 1-3  $\mu\text{m}$  (claimed by the manufacturer). Suppose the diameter  $d$  obeys the log-normal distribution [6]:

$$p(d) d(\ln d) = \frac{1}{\sqrt{2\pi}\sigma} \exp\left[-\frac{(\ln d - \ln d_0)^2}{2\sigma^2}\right] d(\ln d) \quad (7)$$

where  $p(d)$  is the probability density function,  $d_0$  is the median diameter and  $\sigma$  is the standard deviation. To enable 95% of the particle population to be 1-3  $\mu\text{m}$ ,  $d_0 = 1.73 \mu\text{m}$  and  $\sigma = 0.27$ . The size-averaged optical properties were calculated by numerical integration:

$$\bar{X}_\lambda(d_0, \sigma) = \int_0^\infty \bar{X}_\lambda(d) p(d) d(\ln d) \approx \sum_{i=1}^N \bar{X}_\lambda(d) p(d) \Delta_{\ln d} \quad (8)$$

where  $X_\lambda$  stands for a monodisperse spectral property ( $\beta_\lambda$ ,  $\omega_\lambda$ , or  $\Phi_\lambda$ ) and  $\bar{X}(d_0, \sigma)$  is the corresponding sized averaged property. In this case 12 integration points  $d_i$  were selected from 1  $\mu\text{m}$  to 3  $\mu\text{m}$  with a constant log-interval  $\Delta_{\ln d} = d_{i+1} - d_i$ . The original geometric model was linearly enlarged for each opacifier diameter  $d_i$  to calculate the monodisperse spectral properties using MSTM and then averaged over the sizes. The spectral parameters of the opacified aerogel were determined from the individual optical properties of the opacifier and the aerogel and their volume fractions in the material, where the aerogel spectral parameters were calculated as described previously [11]. The resulting optical properties were then used in the DOM to predict the reflectance, where an  $S_{12}$  approximation was used for the anisotropic scattering and the incident boundary conditions were  $\mu_0 = \mu_1$  and  $\varepsilon \rightarrow 0$  to approximate normal incidence.

As shown in Fig. 3, the DOM results based on the MSTM calculation are in better agreement with the measurements than based on Mie theory. The single scattering properties from Mie theory resulted in reflectance predictions higher than the measurement. The comparison verifies the spectral properties shown in Fig. 2 which shows that the surrounding nanoparticles result in stronger absorption and lower albedo of the opacifier. In case that the

errors in Mie results was caused by the fixed opacifier sizes, the calculations were further done with a range of median diameters,  $d_0$ , and standard deviations,  $\sigma$ . Figure 4(a) and 4(b) show that even adjusting the input sizes does not enable the Mie results to agree with the measurements at all wavelengths with the predicted reflectance with showing agreement at short wavelengths (such as  $d_0 = 2.5 \mu\text{m}$  in Fig. 4(b)) but with large errors at long wavelength, and vice versa.

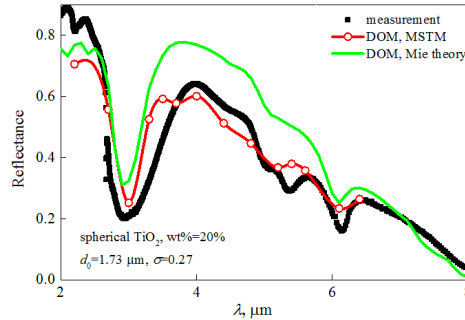


Fig. 3. DOM results from Mie and T-matrix calculations compared with the measured reflectance.

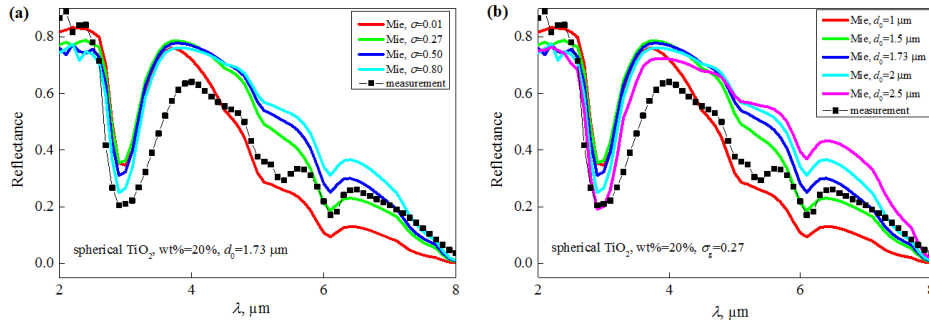


Fig. 4. Size parameters' influence on the Mie results: (a) varied  $\sigma$  with given  $d_0$ ; (b) varied  $d_0$  with given  $\sigma$ .

#### 4. Summary

In this work, the spectral properties of a micrometer-scale opacifier particle surrounded by silica nanoparticles were calculated using the MSTM code based on a computer generated microstructure. This model was validated by comparing the DOM predictions with measured opacified aerogel reflectance. The results show that even the small effect of refraction and scattering by silica nanoparticles affected the optical properties of the opacifier grains inside the aerogel. The absorption efficiency and scattering albedo show observable differences from single scattering properties, while the phase functions are almost unchanged.

The agreement between the theory and experiment also shows the ability of this method to predict the optical and radiative properties. The T-matrix code is useful for systems with large numbers of particles even with extremely different sizes. The discrete ordinate method can be used to predict the radiative properties with known optical parameters and shows satisfactory agreement with measurements.

#### Acknowledgments

This work was supported by the Natural Science Foundation of China (Grant No. 51236004 and 51321002).